URSI - RCRS 2022, IIT (Indore), India, 1 - 4 December, 2022

Study on the role of gravity wave induced perturbations for the sustenance of night time ionospheric plasma irregularities using multi beam HF radar observation in association with ionosonde and GPS data at Thumba

T. V. Sruthi* [1, 2] and G. Manju [1]
[1] Space Physics Laboratory, VSSC, Thiruvananthapuram:695022
[2] University of Kerala, Thiruvananthapuram:695034

Abstract

The role of gravity wave induced seed perturbations for the sustenance of night-time equatorial ionospheric plasma irregularities is studied using multi beam HF radar observations in association with ionosonde and GPSTEC data over Thumba (8.5^0N, 77^0E). HF radar was operated in night mode for 7 days as part of a radar campaign that conducted from the equinoctial period of 30th March to 8th April 2022. Scaling the F layer base height (h'F) based on data from ionosondes provides the post-sunset ionospheric background environment that affects the growth of irregularities. By performing wavelet analysis on GPSTEC data, the amplitude of the gravity wave-induced seed perturbation is retrieved during the sunset hours on all of these days. According to the analysis of seed perturbations and the corresponding h'F data, as altitude drops, the gravity wave amplitude becomes more important for the occurrence of Equatorial Spread F (ESF) irregularity. The current study uses HF radar observations in three beam directions, namely East, West, and Zenith, to examine the contribution of gravity wave amplitude on the sustainability of Spread F irregularity. The duration of the irregularity signal received from the ionosonde has a significant correlation with the full width at half maximum of the gravity wave amplitude. This finding suggests that seed perturbation is necessary not only to initiate ESF irregularities but also to sustain them.

1. Introduction

Equatorial Spread F (ESF) refers to the manifestation of night time ionospheric F region plasma irregularities at magnetic equatorial regions with scale sizes varying from few cms to kms [1, 2]. The satellite-based communication and navigation systems will be severely impacted by nocturnal ionospheric plasma irregularities over the geomagnetic equatorial region. The phase and amplitude of the signals are modified while passing through these irregular structures in the ionosphere. Haerendel [3] proposed the linear theory for the generation of large scale irregularities by the Collisional Rayleigh–Taylor(CRT) instability mechanism. Numerous studies have been conducted on the climatology of the ESF in the Indian and American longitude sectors [4, 5, 6, 7].

The plasma irregularities manifest differently in different instruments. The equatorial plasma irregularities have been studied using ground-based ionosonde, coherent radar, GPS scintillations and optical airglow measurements as well as in-situ satellite and rocket borne measurements [8, 9, 10, 11, 12]. The irregularities develop through RT instability mechanism under certain conducive conditions like the movement of the F-layer to higher altitudes in the post-sunset hours and formation of steep bottom side ionization density gradients. The evening pre reversal electric field enhancement (PRE), which creates a large vertical plasma drift, causes a steep density gradient on the bottom side of the F layer. The effects of meridional winds, in controlling ESF generation, have also been investigated [13]. Devasia [14] have reported that there exists a threshold height (h'F_c) of the base of F layer, above which E × B drift becomes decisive in controlling ESF occurrence regardless of the meridional wind direction. The direction of meridional wind becomes important for the occurrence of ESF irregularities below the threshold height (neutral dynamical regime). When the post sunset h'F (Just before ESF) is below h'F_c, meridional wind polarity needs to be equatorward for ESF to occur. Seasonal and solar cycle variations are seen in the threshold height. The crucial role of gravity wave induced seed perturbations, in the generation of ESF irregularities has been investigated by several workers [15, 16, 17]. Gravity waves that are mainly of lower atmospheric origin can propagate up to ionospheric altitudes if their vertical wavelength is large enough, it can also happen as a result of secondary wave generation when the primary wave breaks in the turbo pause area [18, 19]. Gravity waves will induce perturbations in the ionization density through ion neutral coupling and the induced ionospheric perturbations are known as Travelling Ionospheric Disturbances (TIDs). The gravity wave induced TIDs are significantly influence the day to day variability of Equatorial Spread F [20, 21]. The requisite gravity wave seed magnitudes for ESF triggering are estimated using ionosonde foF_2 data, and threshold curves are generated for magnetically quiet periods while the F layer height was above the threshold height [22] and an empirical model is proposed for predicting ESF for any solar flux and/or post sunset altitude [21]. Bagiya [23] defined a growth factor and this together with perturbation factor is shown as exhibiting control over the evolutionary pattern of ESF irregularities

considering certain days of vernal equinox season of low solar activity. The present study investigates the importance of seed perturbation amplitudes for the sustenance of ESF irregularities using simultaneous measurements of co-located HF radar, ionosonde and GPSTEC data. Further, the gravity wave origin of the perturbations is also unravelled.

2. Data and methodology

The present study made use of multi beam, 18MHz HF radar data over Thumba (8.5^0N, 77^0E) during the equinoctial period from 30th March to 8th April 2022. The radar was operated in night mode for seven days in which 8.3 m scale size irregularity signatures are obtained for five days during the campaign period. The specifications of HF radar operated in multiple beam directions are given in table 2.1. The radar is operated in three switchable beam directions. A zenith beam and the other two beams in east and west directions with zenith angle of 30^0. The in-phase and quadrature- phase outputs (I and Q) signals are subjected to complex FFT. The noise removal is done by subtracting first range gate (where no signal is expected) from all the other gates.
Six Spread F days and one non spread F (NSF) day were identified using co-located simultaneous DPS-4D ionosonde observations. The ESF signatures are manifested first in ionosonde and subsequently in radar. This indicates the evolution of ESF irregularities from large scale size (kilometers) to smaller scale sizes (meters). A day with a range spread of ~30 km in a given ionogram at the frequency of 3 MHz for a duration of more than 30 min is designated as an ESF day, if the irregularities begin to manifest before 21 hr. The background ionospheric condition which influences the development and evolution of ESF irregularities is estimated by scaling base height of F region. The virtual height of the base of the F layer (h'F) is scaled at 2.5 MHz for all these days during evening time. h'F values just before spread F (on ESF days) and at 1900hr (for Non Spread F days) are above the threshold height for all the analyzed days indicating the decisive role of electrodynamics in controlling the ESF occurrence process.

2.1. HF radar system specifications

Operating Frequency	18MHz
Bandwidth	80kHz
Pulse width	100μs
Height resolution, km	15km
Peak power	50kW
Beam direction	zenith, 30°E and 30°W off zenith
Type of antenna	12 × 6 phased dipole array (Mag E-W× N-S)

Calculation of VTEC

The ionosphere is assumed to be a thin layer and the point at which the satellite ray intersects the ionosphere is defined as the Ionospheric Pierce Point (IPP). The measured absolute TEC known as the Slant Total Electron Content (STEC) which depends on the elevation angle of the satellite is converted to Vertical Total Electron Content (VTEC) as follows. Where χ is the angle subtended at the point of intersection of ray path with normal to the earth's surface at height corresponding to IPP.
VTEC = STEC*cos (χ).

An elevation angle cut off of 50° is used such that only points wherein this cut off is exceeded are considered. The wavelet analysis of GPSTEC data on all the days in the campaign is conducted. The mean-removed fluctuations of TEC on each day are subjected to "Morlet" wavelet analysis [24] to assess the amplitude of the gravity-wave induced seed perturbations with 0.5 to 1hr periodicity in the ionosphere. The seed perturbations during 18-18.75 hr. (near the ESF start time ~19 h) are extracted as representative of the post sunset gravity wave induced seed perturbations. An analysis of the perturbation amplitudes extracted in the post sunset hours (18-18.75 hr) with the corresponding h'F data is undertaken.

Gravity wave extraction from HF radar signal

To investigate the importance of gravity wave perturbation amplitude in the sustenance of ESF irregularities, the wave amplitude with 0.5 to 1 hr periodicity is extracted throughout the signal duration by applying wavelet analysis to the temporal variations of mean removed power fluctuations derived from radar. From the altitudinal distribution of the total power at each instant, the maximum value is identified. The temporal evolutions of maximum power values so identified at different instants are interpolated at seven minute interval after the removal of spurious values. There after adjacent averaging is carried out to obtain the overall trend of the data and the trend removed fluctuations are extracted. These fluctuations are subjected to wavelet analysis and temporal evolution of the fluctuation amplitudes are obtained. The full width at half maximum of gravity wave amplitude is correlated with ESF duration obtained from ionosonde. Since the large scale size irregularities will sustain for longer time period compared to those at smaller scale size, the duration of irregularity is measured from ionosonde (which represents km scale size irregularities).

The temporal evolution of mean Doppler frequencies corresponding to above mentioned noise removed power values at two altitudes 387 km and 426 km with significant signal duration are processed to extract the mean removed fluctuations. These fluctuations are also subjected to wavelet analysis and the 0.5-1 hr wave is extracted for both the altitudes.

3. Results and Discussion

3.1 HF radar spectra

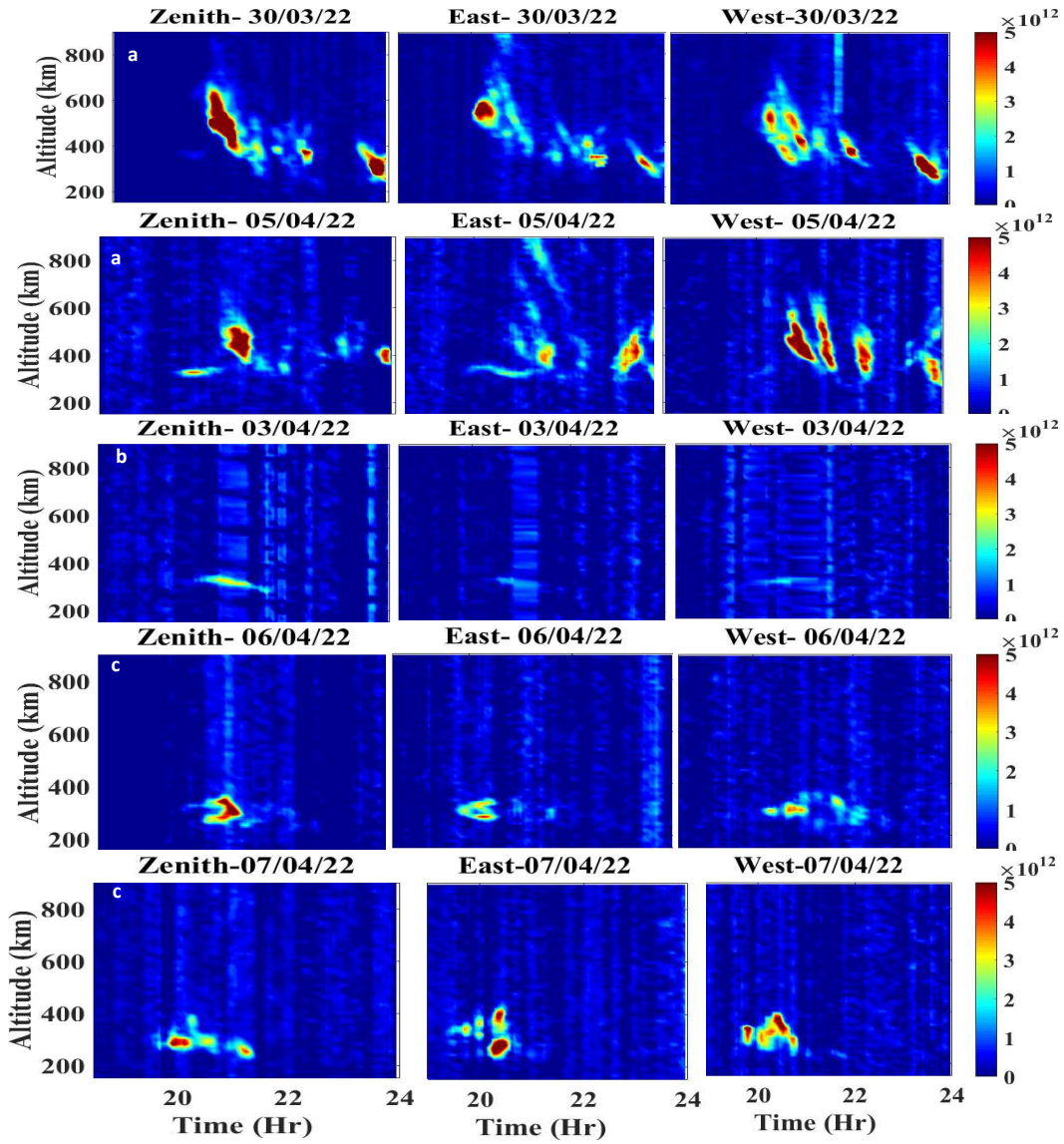

Fig 1.a) Plume structure, b) bottom side structure and c) bottom type structure

Fig 1 shows the ESF irregularity signature observed using 18 MHz HF radar operated in three different beam directions (zenith, east and west). These observations of nighttime F region irregularities made by HF radar at geomagnetic equatorial station shows plume structures, bottom-type and bottom-side irregularity structures. Similar kind of irregularity structures have been reported earlier, at off equatorial station Gadanki (13.5^{0}N, 79.2^{0}E) using Gadanki Ionospheric Radar Interferometer (GIRI) [25]. Of the 5 geomagnetically quiet days (Ap<18) with nocturnal radar signal returns, plume structure was evident in the case of 2 days (30th March and 5th April) (Fig 1.a), while bottom side structure (Fig 1.b) was obtained on 1 day (3rd April) and bottom type structure (Fig 1.c) manifested on 2 days (6th and 7th April). Clear periodic modulations are observed in the radar echoes in all three beam directions as is evident in figure. Plume structures initially manifested at lower altitudes and thereafter evolved to higher altitudes before drifting downwards to reach altitudes around 250 km close to midnight. In Fig 1.b the irregularities are constrained only to lower altitude regions like a thin layer. The bottom type irregularities are developed in the lower altitude and slightly evolve to higher region, but not as high as plume structures.

3.2 Post sunset ionospheric condition

Fig 2. shows the temporal variation of h'F in the evening time. The post sun set ionospheric F layer height is one of the important parameters that controls the generation of nighttime irregularity structures. The PRE associated post sunset height rise is evident in this figure. The threshold height for low solar activity period is reported as 243km [6]. The h'F just before spread F and at 1900hr (for NSF days) are above the threshold height for all these days. This clearly indicates the role of electrodynamical processes in ESF occurrence [14]. For non-spread F day (31march 2022) the F layer was at a comparatively lower altitude (299km). During one of the strong spread F days 30 March 2022 the layer as seen in ionosonde, reaches up to 400km.

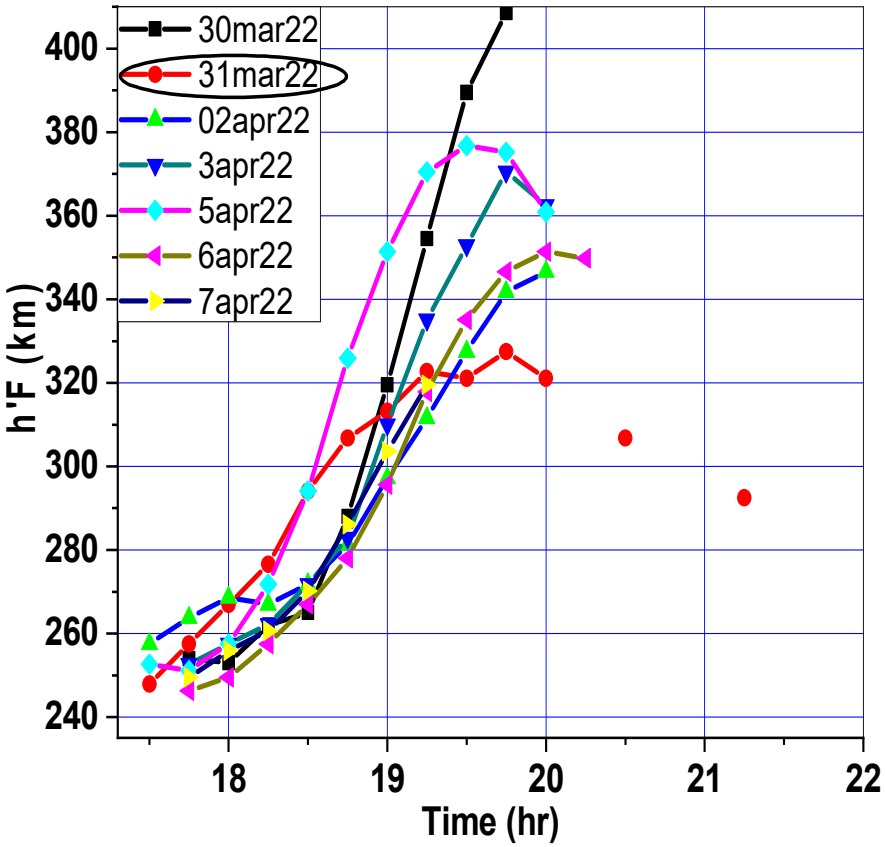

Fig2. The temporal variation of h'F in the evening time

3.2 Effect of Precursor perturbations from GPSTEC data and h'F on ESF triggering

The seed perturbation amplitude extracted in the post sunset hours (18-18.75 hr) by doing wavelet analysis of temporal variations of GPSTEC data is analyzed with the corresponding h'F data for all these days. Fig 3 shows the variation of seed perturbation with h'F. The analysis reveals that for all the days when the layer was at very high altitudes (337 km), ESF manifested irrespective of the ambient seed perturbation amplitude in the post sunset hours. Whereas, for the two days with F layer altitude below 300 km, ESF occurred for the day with significantly higher gravity wave amplitude. The requisite seed

perturbation for ESF occurrence increases as altitude decreases. This is in agreement with the previous result [20, 21] indicating that gravity wave amplitude is critical for ESF occurrence as the altitude decreases.

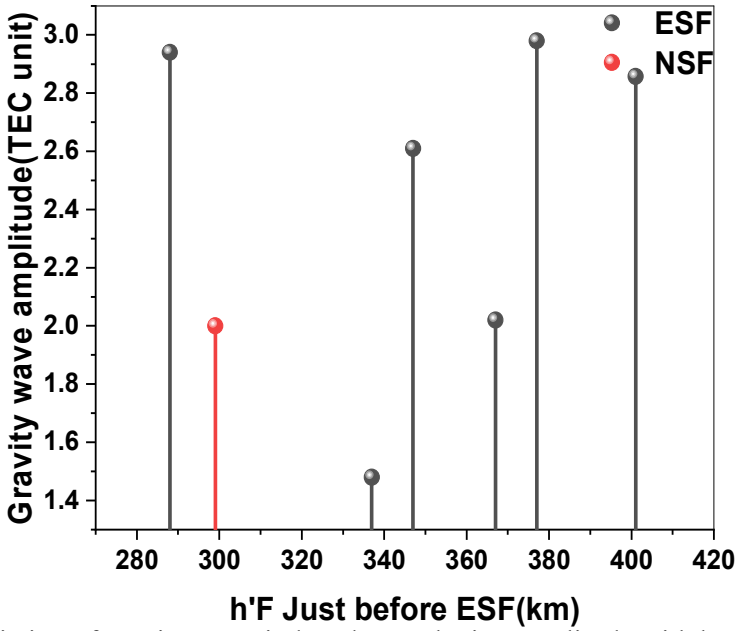

Fig 3. Variation of gravity wave induced perturbation amplitude with h'F just before ESF

3.3 a) Effect of persistence of perturbations derived from HF radar data on ESF sustenance

It is well understood that an initial seed perturbation is needed for triggering Rayleigh-Taylor instability which will lead to the development of large scale irregularities in the night time F region altitude. The present study investigates the role of gravity wave amplitude for the sustenance of Spread F irregularity using HF radar observations in three beam directions, viz., East, West and Zenith. Previous studies have shown that gravity waves in the period range of 0.5 -1 hr [20, 21] are capable of seeding the equatorial spread F irregularities. Perturbations with periodicities of 0.5to 1hr are extracted by applying wavelet analysis over temporal variation of mean removed power fluctuations from radar. The full width at half maximum (FWHM) of gravity wave amplitude is correlated with irregularity signal duration estimated from ionosonde observations.

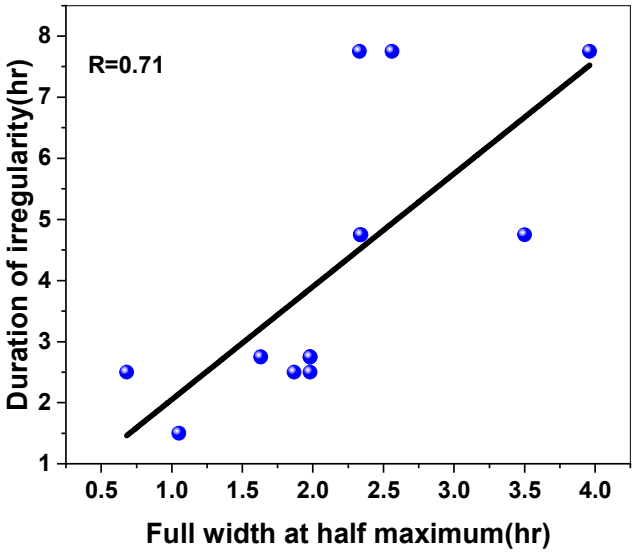

Fig 4. Correlation between FWHM of gravity wave amplitude and duration of ESF irregularity

Fig 4 shows the correlation between FWHM of gravity wave amplitude and duration of ESF irregularity. It is evident from the figure that full width at half maximum of gravity wave amplitude extracted from radar power shows significant correlation (R=0.71) with duration of irregularities. The significance of this correlation is found to be 99% as per the t test. This result indicates the requirement of seed perturbation not only for triggering Rayleigh-Taylor instability but for the

persistence of ESF irregularities as well. This is probably due to the fact that in the late night periods the layer already moves to much lower altitudes where electrodynamics becomes progressively unfavorable for RT instability and hence the seed requirement will be very critical for sustenance of irregularity.

3.4 b) Analysis on gravity wave origin of the seed perturbations

An analysis of the possible gravity wave origin of the seed perturbations is also carried out using temporal variations of mean Doppler frequencies at two altitudes. Fig 5.a top panel shows the temporal variation of mean Doppler frequencies at 387 km along with the smoothed trend (3 point adjacent averaging) of the Doppler variations, while the corresponding mean removed fluctuations are depicted on the bottom panel. Fig 5.b shows the same as Fig 5.a but for 426 km. The temporal variations of the fluctuations at 387 km and 426 km are subjected to wavelet analysis and the real part of the 0.5- 1 hr wave components are extracted. Fig. 6 depicts the variations of the 0.5-1 hr wave component at 387 km and 426 km. The features of upward amplitude propagation and downward phase propagation are patent from the figure thereby confirming the gravity wave origin of the perturbations.

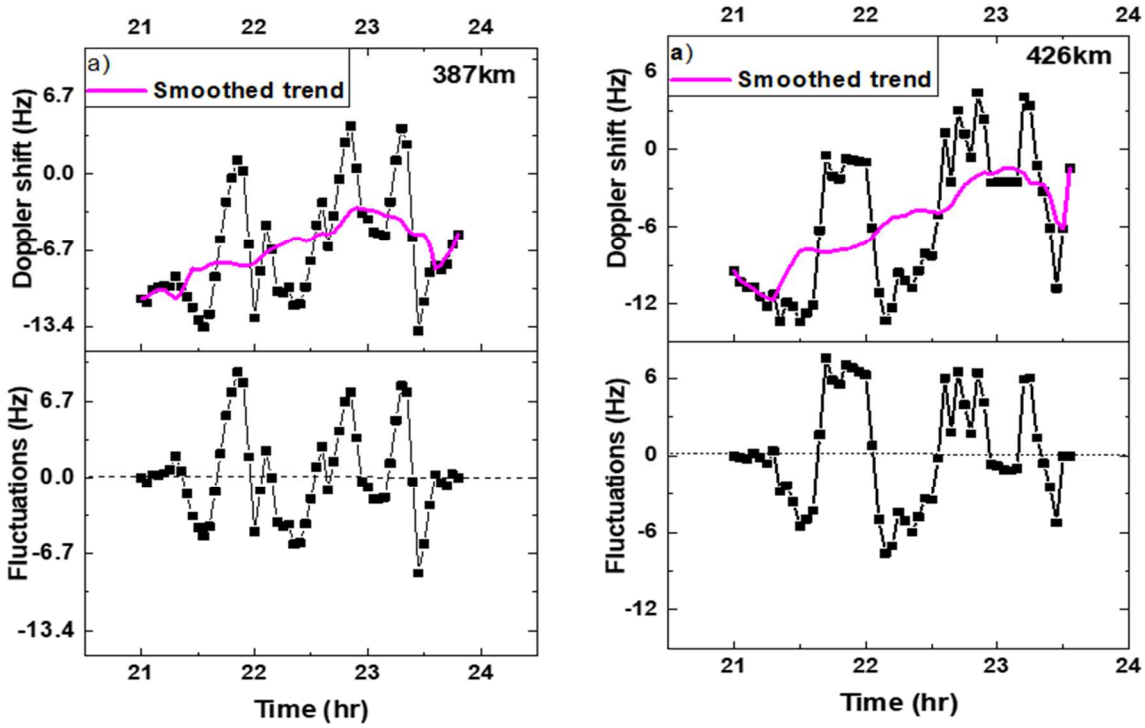

Fig 5.a The temporal variation of mean Doppler frequencies at 387 km along with the smoothed trend (top panel) and mean removed fluctuations (bottom panel). **Fig 5.b** the temporal variation of mean Doppler frequencies at 426 km along with the smoothed trend (top panel) and mean removed fluctuations (bottom panel).

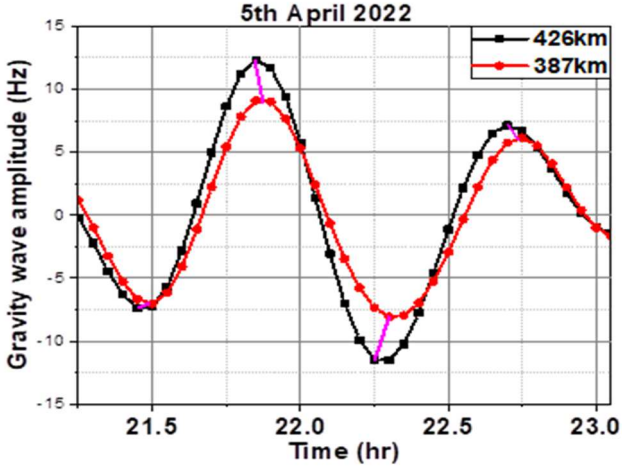

Fig. 6 Wave components of the (0.5-1) hr wave for the altitudes 387km and 426 km.

4. Conclusion

The seed perturbation amplitude is a critical parameter for ESF irregularity occurrence. This study reveals that the seed perturbation amplitude is necessary not just for initial triggering of ESF but for the sustenance of irregularity as well. The FWHM of gravity wave amplitude exhibit significant correlation (99%) with the duration of irregularities. The gravity wave origin of the seed perturbations is also brought out in the study.

5. Acknowledgements

The authors gratefully acknowledge the support and research opportunity provided by Indian Space Research Organization (ISRO) for this work. The authors thank Dr. Rajkumar Choudhary, PI, INSWIM project, SPL for providing GPS data. We also express our gratitude to members of Atmospheric Technology Division of SPL, for radar related technical support.

6. References

1. R. F. Woodman and C. La Hoz, "Radar observations of Fregion equatorial irregularities," *Journal of Geophysical Research*, **81**, 31, November 1976, pp. 5447–5466, doi: 10.1029/JA081i031p05447.
2. D. T. Farley, B. B. Balsey, R. F. Woodman, and J. P. McClure, "Equatorial spread F: Implications of VHF radar observations," *Journal of Geophysical Research*, **75**, 34, December 1970, pp. 7199–7216. doi: 10.1029/JA075i034p07199.
3. G. Haerendel. ''Theory of equatorial spread F'', Max-Planck Institute for Physics and Astrophysics, Garching, Germany.1974.
4. K. S. V. Subbarao and B. V. K. Murthy, "Post-sunset F-region vertical velocity variations at magnetic equator," *Journal of Atmospheric and Terrestrial Physics*, **56**, 1, Jan. 1994, pp. 59–65, doi: 10.1016/0021-9169(94)90176-7.
5. M. A. Abdu, "Coupling and energetics of the equatorial ionosphere-thermosphere system: advances during the STEP period," *Journal of Atmospheric and Solar-Terrestrial Physics*, **61**, 1–2, January 1999, pp. 153–165, doi: 10.1016/S1364-6826(98)00125-4.
6. G. Manju, C. V. Devasia, and R. Sridharan, "On the seasonal variations of the threshold height for the occurrence of equatorial spread F during solar minimum and maximum years," *Annales Geophysicae*, **25**, 4, May 2007, pp. 855–861, doi: 10.5194/angeo-25-855-2007.
7. M. K. Madhav Haridas, G. Manju, and T. Arunamani, "Solar activity variations of equatorial spread F occurrence and sustenance during different seasons over Indian longitudes: Empirical model and causative mechanisms," *Advances in Space Research*, **61**, 10, May 2018, pp. 2585–2592, doi: 10.1016/j.asr.2018.02.040.
8. A. K. Patra, P. B. Rao, V. K. Anandan, and A. R. Jain, "Radar observations of 2.8 m equatorial spread-F irregularities," *Journal of Atmospheric and Solar-Terrestrial Physics*, **59**, 13, September 1997, pp. 1633–1641, doi: 10.1016/S1364-6826(96)00162-9.
9. A. Bhattacharyya, S. J. Franke, and K. C. Yeh, "Characteristic velocity of equatorial F region irregularities determined from spaced receiver scintillation data," Journal of *Geophysical Research*, **94**, 9, 1989, pp. 11959, doi: 10.1029/JA094iA09p11959.
10. M. Mendillo and J. Baumgardner, "Airglow characteristics of equatorial plasma depletions," *Journal of Geophysical Research*, **87**, 9, 1982, p. 7641, doi: 10.1029/JA087iA09p07641.
11. H. S. S. Sinha, S. Raizada, and R. N. Misra, "First simultaneous in situ measurement of electron density and electric field fluctuations during spread F in the Indian Zone," *Geophysical Research Letters*, **26**, 12, June 15, 1999, pp. 1669–1672, doi: 10.1029/1999GL900339.
12. W. J. Burke, "Longitudinal variability of equatorial plasma bubbles observed by DMSP and ROCSAT-1," *Journal of Geophysical Research*, **109**, 12, 2004, doi: 10.1029/2004JA010583.
13. T. Maruyama and N. Matuura, "Longitudinal variability of annual changes in activity of equatorial spread F and plasma bubbles," *Journal of Geophysical Research*, **89**, 12, , 1984, p. 10903, doi: 10.1029/JA089iA12p10903.
14. C. V. Devasia, N. Jyoti, K. S. V. Subbarao, K. S. Viswanathan, D. Tiwari, and R. Sridharan, "On the plausible linkage of thermospheric meridional winds with the equatorial spread F," *Journal of Atmospheric and Solar-Terrestrial Physics*, **64**, 1, January 2002, pp. 1–12, doi:10.1016/S1364-6826(01)00089-X.
15. R. T. Tsunoda, "On seeding equatorial spread during solstices," *Geophysical Research Letters*, **37**, 5, March 2010, doi: 10.1029/2010GL042576.
16. R. T. Tsunoda, "On equatorial spread F: Establishing a seeding hypothesis," *Journal of Geophysical Research: Space Physics*, **115**, 12, December 2010, doi: 10.1029/2010JA015564.
17. J. D. Whitehead, "Ionization disturbances caused by gravity waves in the presence of an electrostatic field and background wind," *Journal of Geophysical Research*, **76**, 1, January 1971, pp. 238–241, doi: 10.1029/JA076i001p00238.
18. S. L. Vadas and D. C. Fritts, "The importance of spatial variability in the generation of secondary gravity waves from local body forces", *Geophysical Research Letters*, **29,** (20), 2002, pp.45-1, doi: 10.1029/2002GL015574.

19. S. L. Vadas, D. C. Fritts, and M. J. Alexander, “Mechanism for the generation of secondary waves in wave breaking regions”, *Journal of the Atmospheric Sciences*, **60**(1), 2003, pp.194-214, doi: 10.1175/1520-0469.
20. R. P. Aswathy and G. Manju, “Gravity wave control on ESF day-to-day variability: An empirical approach,” *Journal of Geophysical Research,* **122**, 2017, pp. 6791–6798, doi: 10.1002/2017JA023983.
21. R. P. Aswathy and G. Manju, “Hind casting of equatorial spread F using seasonal empirical models,” *Journal of Geophysical Research: Space Physics,* ***23***, 2018, pp. 1515–1524, doi: 10.1002/2017JA025036.
22. G. Manju, M. K. Madhav Haridas, and R. P. Aswathy, “Role of gravity wave seed perturbations in ESF day-to-day variability: A quantitative approach,” *Advances in Space Research*, **57**, 4, February 2016, pp. 1021–1028, doi: 10.1016/j.asr.2015.12.019.
23. M. S. Bagiya and R. Sridharan, “Evolutionary phases of equatorial spread F including L band scintillations and plumes in the context of GPS total electron content variability: A case study,” *Journal of Geophysical Research: Space Physics*, **116**, 10, October 2011, doi: 10.1029/2011JA016893.
24. C. Torrence, and& G. P. Compo,” A practical guide to wavelet analysis”, *Bulletin of the American Meteorological Society*, **79**, 1998, pp. 61 –79, doi.: 10.1175/1520-0477.
25. A.K. Patra, P. Srinivasulu, P. P. Chaitanya, M. D. Rao, and A. Jayaraman, “First results on low-latitude E and F region irregularities obtained using the Gadanki Ionospheric Radar Interferometer”, *Journal of Geophysical Research: Space Physics*, **119**(12), 2014, pp.10-276, doi:10.1002/2014JA020604.